PHYSICAL REVIEW B VOLUME 24, NUMBER 2 15 JULY 1981

# The surface photoeffect

Harry J. Levinson* and E. W. Plummer
*Department of Physics, University of Pennsylvania, Philadelphia, Pennsylvania 19104 and Laboratory for Research on the Structure of Matter, University of Pennsylvania, Philadelphia, Pennsylvania 19104*
(Received 22 December 1980)

Angle-resolved photoelectron spectroscopy coupled with the polarized continuum of synchrotron radiation has been used to identify unambiguously a large enhancement in the photoexcitation from Al(100) due to the surface photoeffect. This large enhancement in the cross section occurs only when the excitation field has a component perpendicular to the surface and is due to the dielectric response in the surface region, i.e., to the spatially varying electromagnetic field at the metal surface. An absolute determination of the differential photoionization cross section for excitation of Fermi-energy electrons shows quantitative agreement with Feibelman's self-consistent calculation. A simple picture of the surface photoeffect will be presented.

## I. INTRODUCTION

Photoemission has proven to be a very useful probe of the electronic wave functions at the surface of a solid. The photoemission intensity will depend strongly upon the nature of the radiation field in the surface region. The discontinuity in the electromagnetic field which appears at the vacuum-solid interface in a macroscopic model of dielectric responce will on a microscopic level become a continuous but rapidly varying field. This spatially varying field, induced by the dielectric response of the surface region, can be the major contributor to "surface photoemission." We have identified the effects on the photoemission intensity from Al(100) due to the spatially varying photon field at the surface.[1]

A useful starting point for this discussion is the photoionization matrix element[2]

$$M_{fi} = \langle f \mid \vec{A}_0(\vec{r})\cdot\vec{p} + \vec{p}\cdot\vec{A}_0(\vec{r}) \mid i \rangle \qquad (1)$$

where $\vec{p} = -i\hbar\vec{\nabla}$ is the momentum operator, $\vec{A}_0(\vec{r})$ is the vector potential of the incident radiation field, and $|i\rangle$ and $|f\rangle$ are the exact initial and final states of the unperturbed system, respectively. Frequently Eq. (1) is manipulated into the form[2]

$$M_{fi} = 2\langle f \mid \vec{A}_0(\vec{r})\cdot\vec{p} \mid i \rangle - i\hbar\langle f \mid (\vec{\nabla}\cdot\vec{A}_0(\vec{r})) \mid i \rangle . \qquad (2)$$

In the gauge chosen $\vec{\nabla}\cdot\vec{A}_0 = 0$ for light propagating through a vacuum, so the second term vanishes. A nonzero divergence of the vector potential implies the existence of longitudinal electromagnetic waves or rapidly varying transverse fields. Such fields may exist only in the presence of sources of electric fields, i.e., in matter.

The direct replacement of the exact many-body states in Eq. (1) by their corresponding approximate single-particle wave-functions will produce incorrect values for the photoemission cross sections when many-body effects are significant. It is important to recognize that, just as the approximate eigenstates of the unperturbed system are found in some appropriate average potential, the perturbing field $\vec{A}(\vec{r})$ that an electron in a single-particle state "sees" must also be some average effective field.[3] The correct prescription then for evaluating the photoionization matrix element is to replace the incident field $\vec{A}_0$ in Eq. (1) with a field which includes the dielectric response of the system to $\vec{A}_0$. This picture of photoemission maintains the single-particle nature of the matrix element by *incorporating many-body effects into an effective field.* What is of importance for photoemission is that the dielectric response of the surface region is fundamentally different from that of the bulk, because of the rapid change in the charge density.

In the ultraviolet and soft-x-ray portions of the electromagnetic spectrum, the wavelength of the light in vacuum ($60 \lesssim \lambda \lesssim 1200$ Å) is much longer than atomic dimensions. The transverse field in the bulk of the solid is also long wavelength. On the other hand, the induced field in the surface region may be varying rapidly. The classical Maxwell field changes from its vacuum to bulk value over a distance short compared to the wavelength of the light. It has long been known that this transition of the fields at the surface does not necessarily occur in a simple monotonic fashion.[4,5] The following two illustrations point out the possible behavior of the effective field at the surface. If the dielectric response of

 ©1981 The American Physical Society

the surface is characterized by a local frequency-dependent dielectric constant $\epsilon(z,\omega)$, where $z$ is the distance from the surface, the normal component of $\vec{A}(\vec{r})$ is found[4,5] to behave as $1/\epsilon(z,\omega)$ for incident light polarized. When the bulk dielectric $\epsilon(z \rightarrow \infty,\omega)$ is negative, there will be some point in the surface region for which $\epsilon(z,\omega) = 0$, causing a singularity. An imaginary contribution to the bulk dielectric constant will soften the singularity in the field into a peak. For $\epsilon(z \rightarrow \infty,\omega) > 0$ the fields will change monotonically from their vacuum to bulk values but still vary rapidly over distances shorter compared to the wavelength of the light in vacuum. When the incident light is $s$ polarized the field is nearly constant in the surface region,[4] in contrast to the situation for $p$ polaraization.

The second consideration is the oscillating charge density $\rho$ at the surface caused by $\vec{\nabla}\cdot\vec{E} = 4\pi\rho \neq 0$. This oscillating charge will induce a longitudinal field in the metal.[6] When the photon energy is greater than the bulk plasmon energy $\hbar\omega_p$ these longitudinal fields will be propagating bulk plasmons, while below $\hbar\omega_p$ these fields will be limited to the surface region.[7] These longitudinal surface[6] waves must be treated in a nonlocal dielectric response model.

In this paper we will present data which will unambiguously show that dielectric response plays a significant role in determining the intensity of photoionization. In certain spectral regions the second term in Eq. (2) [with $\vec{A}_0$ replaced by the effective Maxwell field $\vec{A}(\vec{r})$] will actually be the dominant one. This will result from the peak in the radiation field in the surface region discussed earlier which occurs for photon energies less than $\hbar\omega_p$ [$\epsilon(z \rightarrow \infty,\omega) < 0$]. We see no identifiable effects on photoemission due to the induced longitudinal fields described above.[1]

In order to see how one may experimentally determine the effect on photoemission due to a spatially varying photon field in the surface region it is useful to look again at the photoemission matrix element. There are three contributions to a photoionization cross section: the initial state, final state, and the photon field. The use of energy- and angle-resolved photoemision allows one to separate many of the effects due to the different contributions. An effect caused by a single-particle final state will occur at a fixed kinetic energy, while an effect due to the photon field will occur at a fixed photon energy. Accordingly, sturcture in the intensity of photonionization for different initial states at a given photon energies will be due to the photon field.

## II. DATA

Earlier efforts to confirm experimentally the existence of this spatially varying photon field have consisted primarily of measurements of total photoelectric yields, that is, the total electron currents emitted from illuminated samples, as a function of photon energy and its polarization.[8–17] These measurements of total photoyields have demonstrated the inadequacy of a simple isotropic volume theory[18,19] in explaining photoemission from solids and have also shown the significant role of surface plasmons in photoexcitation from rough films.[10,14–16] However, the interpretation of total photoyield measurements is always ambiguous because many of the physical processes determining the photoyield are not well understood.

A smooth aluminum (001) surface was studied to circumvent problems which result from surface roughness. In order to avoid the ambiguities inherent in total photoyield measurements we have used energy- and angle-resolved photoelectron spectroscopy to study the effect of dielectric response on photoemission. A single-crystal sample, along with the energy- and angle-resolved detection, meant that well-defined initial and final states were involved in a given measurement, again reducing ambiguity. Aluminum was chosen because it is a relatively simple metal for which electron gas models should be applicable.

The data were taken with a constant transmission spectrometer which had an angular resolution of $\pm 2.5°$ and energy resolution which could be varied.[20] The synchrotron radiation from the University of Wisconsin Tantalus I storage ring was dispersed by a 1-m Seya-Namioka monochromator with fixed slits, so that the combined energy resolution varied between $\sim 0.2$ and 0.3 eV as the photon energy was increased from 9 to 30 eV. The polarization of the light exiting the monochromator was estimated to be $> 96\%$. The photon flux was monitored by an NBS $Al_2O_3$ photodiode[22] and sodium salicylate. The latter was more accurate at the lower photon energies while the photodiode provided an absolute calibration of the photon flux.

The aluminum (001) crystals were oriented by Laue diffraction and spark planed to within 0.5° of the desired surface. The crystals were polished with successively finer grits of alumina, down to 0.05-$\mu$m sized grit, and further mechanically polished with Syton 30,[23] a suspension of 40-nm silica particles. This led to a much smoother and flatter surface than we could obtain by electropolishing or eva-

porating a film. The crystals were cleaned in vacuum by repeated ion bombardment and annealling at 375°C. In order to remove the thick oxide layer, the ion energies were initially 800 eV but were lowered to 600 eV when the oxide was reduced to a few layers in order to minimize surface damage. All of the data refer to crystals which had less than a few percent of a monolayer of oxygen on the surface, except where noted.

Typical normal emission energy distribution curves are shown in Fig. 1. The prominent features in the data are the Fermi edge and a surface-state peak at 2.75-eV-lower binding energy.[24,25] It is clear from these curves that the dominant contribution to the total photoyield comes from the low kinetic energy, inelastically scattered electrons which originate, for the most part, in the bulk. Only at low photon energies, where the reflectivity is high, does the secondary background become small. This illustrates one difficulty in separating "bulk" and "surface"contributions to the total photoyield. Energy-resolved detection allows one to distinguish between scattered and unscattered electrons to an extent sufficient to circumvent this problem. Because of the short photoelectron mean free path (5 — 10 Å),[26] unscattered electrons must originate in the surface region.Thus, our measurements are surface-sensitive.

The intensity of photoionization from the Fermi level as a function of photon energy for normally incident *s*-polarized light and off normal emission, normalized to the number of incident photons, is shown in Fig. 2. $k_{||}$ was constant at 0.61 $Å^{-1}$ along the $\bar{\Gamma} \rightarrow \bar{X}$ direction in the surface Brillouin zone ($k_{||} = 1.1$ $Å^{-1}$ at $\bar{X}$). The photoemission intensity for this experimental geometry is rather weak as indicated by the scatter in the data. The cross section nevertheless exhibits a maximum between 14 and 16 eV photon energy, which was quite reproducible. This peak lies near the bulk plasmon energy at 15 eV. The solid curve in Fig. 2 is the square of the classical transverse Fresnel vector potential at the surface, which has been computed from measured optical constants.[27,28] The photoemission intensity follows the classical fields when $\vec{A}$ is parallel to the surface, as anticipated. This suggests that the single-particle matrix element

$$\langle f \,|\, \hat{e}_A \cdot \vec{p} \,|\, i \rangle \ ,$$

where $\hat{e}_A$ is a unit vector in the direction of $\vec{A}$, does not vary rapidly in this photon energy range. It will be shown later that this is indeed the case.

The Fermi-level photoionization cross section for *p* polarized incident light with the same collection geometry as Fig. 2 is shown in Fig. 3. All cross sections presented in this paper are plotted in the same units, the absolute normalization being discussed at the end of this section. The cross sections for the two different polarizations of the incident light differ in magnitude and behavior as a function of photon energy. Well below $\hbar\omega = 15$ eV, the photoionization intensity is more than an order of mag-

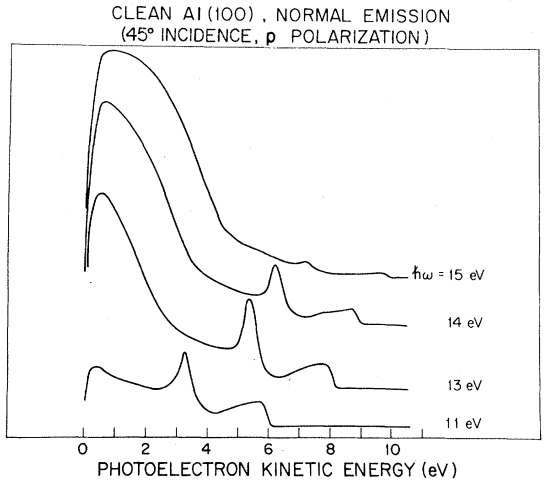


FIG. 1. Typical normal emission energy distribution curves normalized to the incident photon flux. The incident light was *p*-polarized and 45° incident. The $\vec{A}$ vector of the photon field was in the (110) mirror plane (direction $\bar{\Gamma} \rightarrow \bar{X}$ in the surface Brillouin zone).

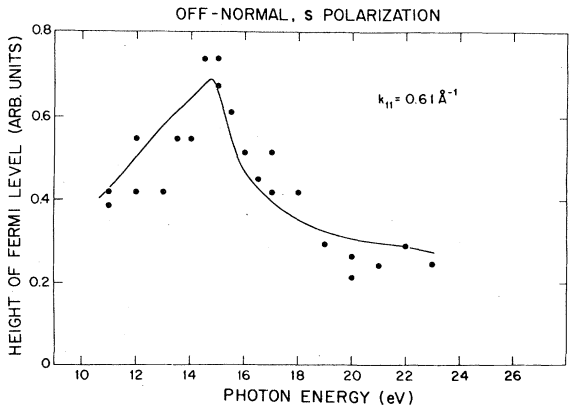


FIG. 2. Fermi level ($k_{||} = 0.61$ $Å^{-1}$ between $\bar{\Gamma}$ and $\bar{X}$) for normally incident, *s*-polarized light. The $\vec{A}$ vector of the photon field was in the (110) mirror plane as was the detector. The solid curves are the classical values of $|\vec{A}|^2$ at the surface, calculated from measured optical constants.[27,28]

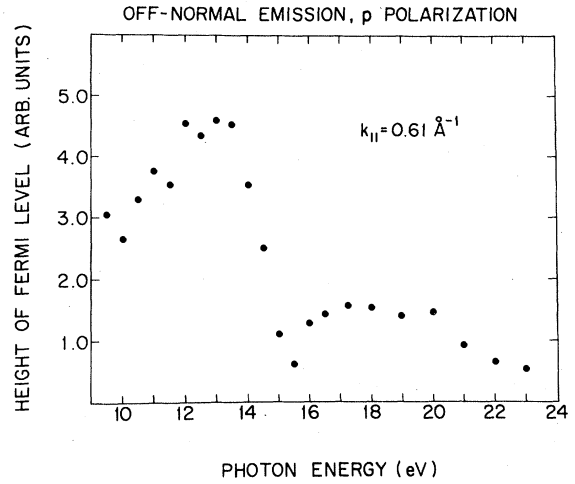


FIG. 3. Fermi level ($k_{||} = 0.61$ Å$^{-1}$ along $\bar{\Gamma}$ to $\bar{X}$) photoionization cross-section for $p$-polarized incident light. The $\vec{A}$ vector was in the (110) mirror plane and the collection geometry was the same as for the data in Fig. 2.

nitude larger when the photon field has a component perpendicular to the surface. The cross section for $p$-polarized light has a minimum near the position for the maximum in the data for $s$ polarization. In this spectral region, within a few volts of 15 eV, the data for the two different polarizations of the incident light have nearly the same magnitude. The two sets of data differ in intensity much more below $\hbar\omega = 15$ eV than at the higher photon energies.

In contrast to the data for $s$-polarized incident light (Fig. 2), the frequency dependence of the cross sections for $p$-polarized light cannot be explained in terms of the Fresnel fields, which are shown in Fig. 4. The classical transverse fields have a discontinuity at the surface when the light has a vector component normal to the surface. Therefore two fields must be considered, one just "outside" the nominal surface and one just "inside." These two fields differ in magnitude by a factor of $|\epsilon|$, where $\epsilon$ is the bulk dielectric constant. In the spectral range currently being considered, the perpendicular component inside the solid is much larger at the higher photon energies compared to $\sim$ 12 eV, and it does not have a minimum near 15 eV, in contrast to the data. The field outside the metal does have a minimum at 15 eV but is also larger at the higher photon energies than at the lower energies. It also seems rather peculiar to describe the photoemission intensity of a bulk state in terms of the field "outside" the metal. In any case, the spectral profile of the data is not simply described by the transverse Fresnel field when the incident light has a component perpendicular to the surface.

While there are clear differences in the behavior of the data for $s$- and $p$-polarized excitation fields, it is not possible to assume unequivocally that the difference are attributable to spatial variations in the

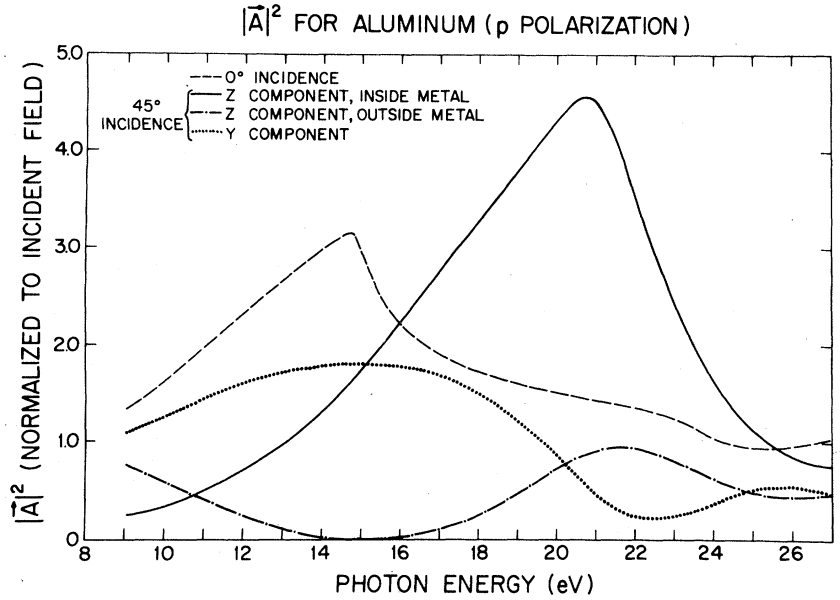


FIG. 4. The square of the vector potential of the classical Fresnel fields, calculated from measured optical constants (Refs. 27 and 28).

photon field. This may be seen as follows. Suppose that it is possible to account for the many-body response in terms of the long-wavelength macroscopic fields, and all other properties of the system may be adequately described in a single-particle picture. Then the photoemission cross section from an initial state $|i\rangle$ to a final state $|f\rangle$ is given by

$$\frac{d\sigma}{d\Omega} \propto |\vec{A}|^2 |\langle f | \hat{e}_A \cdot \vec{\nabla} V(\vec{r}) | i \rangle|^2 \ . \tag{3}$$

$\vec{A} = A\hat{e}_A$ is the vector potential of the field at the sample and $V(\vec{r})$ is the crystal potential and surface barrier. Preferential photoemission in the direction of the excitation field is common for atoms and molecules.[29] When this occurs in a solid the observed photoyields are larger for $p$-polarized light since more photoelectrons are then directed out of the solid. Such an anisotropic volume effect is known to account for at least part of the difference between the total photoyield for $s$- and $p$-polarized excitation fields.[19,30–33] Since aluminum is a nearly-free-electron metal the contribution to $\vec{\nabla} V(\vec{r})$ from the ion cores is expected to be weak, the dominant contribution arising from the surface potential barrier. This results in stronger surface photoexcitation by field components perpendicular to the surface than parallel to the surface. Moreover, there is no reason to expect the cross section to behave as $|\vec{A}|^2$ as a function of photon energy even in a single-particle model. In order for this to occur, the matrix element

$$\langle f | \hat{e}_A \cdot \vec{\nabla} V(\vec{r}) | i \rangle \tag{4}$$

must remain constant as the photon energy, and therefore $|f\rangle$ is varied. There is no *a priori* reason why this should occur, but it appeared to be the case for $s$-polarized light shown in Fig. 2.

It should be noted that a proper comparison of the photoexcitation due to $s$- and $p$-polarized light should be made at a fixed angle of incidence. For low photon energies and non-normal angles of incidence, the transmitted wave is refracted along the surface (Fig. 5). Because of the short photoelectron mean free paths, such strongly refracted waves would result in greater photoemission intensities than would a wave of the same amplitude which propagates away from the surface. Unfortunately, the manipulator used for these experiments allowed for $s$-polarized light only at normal incidence, preventing a clear comparison between $s$- and $p$-polarized photoexcitation. Nevertheless, there are dramatic differences between the two modes of excitation and they can be understood independently of each other.

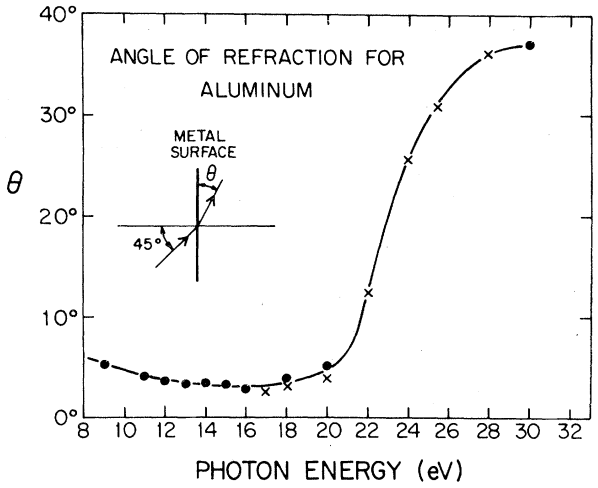


FIG. 5. Classical angle of refraction from Snell's law. The circles were calculated with the data of Ref. 28, while the $\times$'s were obtained using the data of Ref. 27. For photon energies $\lesssim$ 22 eV, the light is refracted within $\sim$ 5° of the surface.

The marked differences between the photoionization cross sections for $s$- and $p$-polarized incident radiation fields certainly indicates an effect on photoemission due to a spatially varying photon field in the surface region. However, since some differences are expected even in a single-particle picture, this conclusion remains tentative. By looking at different initial states in the same experimental geometry we have been able to separate single-particle matrix elements to a certain extent.

Normal-emission photoionization cross sections for the Fermi level and surface state are shown in Fig. 6. The incident light for these data is $p$-polarized. The angle- and energy-resolved capabilities of our spectrometer allow for a clear separation for bulk and surface effects and photoexcitation due to the components of the photon field parallel and perpendicular to the surface. At $k_{||} = 0$ (normal emission) the states at Fermi level and the surface state are symmetric with respect to all symmetry operations of the surface. The data presented in this paper for $p$-polarized incident light were taken with the $y$ component of the photon field perpendicular to a symmetry plane. Accordingly, only the component of the field normal to the surface results in photoexcitation. The short inelastic mean free paths for the photoelectrons result in surface sensitivity since only unscattered electrons contribute to the measured Fermi-level and surface-state cross sections.

Both states have roughly the same spectral profile

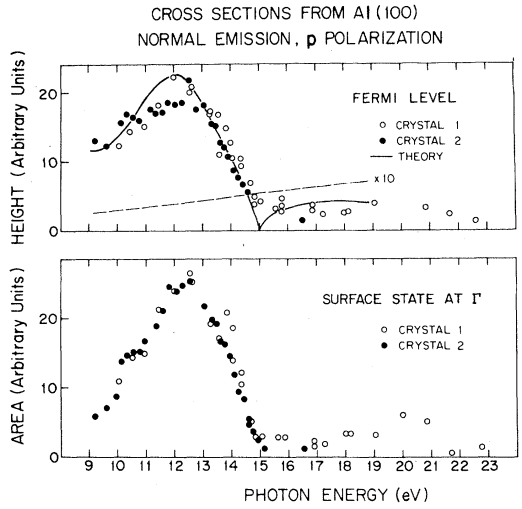


FIG. 6. The circles are the measured Fermi-level and surface-state normal-emission cross sections for light 45° incident, the $\vec{A}$ vector in the (110) mirror plane. The solid curve is the Fermi-level cross section from jellium calculated with self-consistently determined electromagnetic fields. The dashed line is the single-particle cross section obtained with an excitation field of unit amplitude everywhere in space. The $r_s = 2$ jellium calculations are plotted as functions of $\hbar\omega/\hbar\omega_p$, where $\hbar\omega_p$ is renormalized to the measured plasmon energy of 15 eV. The magnitude of the measured and calculated cross sections were normalized at 13 eV. A further discussion of the intensities is given in the text.

and resemble the data in Fig. 3. The cross section is relatively intense at threshold, rises to a maximum value between 12 and 13 eV, falls rapidly to a minimum near 15 eV, and remains small at higher photon energy. Since the different states have the same spectral profile, the behavior of the data as a function of photon energy is not peculiar to one initial-state wave-function. The data in Fig. 6 also enables one to eliminate final-state effects as the source of the intense photoemission below $\hbar\omega_p = 15$ eV. A final-state resonance should give a peak in the photoionization cross section at fixed *kinetic* energy while the peak in the data in Fig. 6 occurs at fixed *photon* energy. Given the 2.75-eV difference in binding energy between the Fermi level and the surface state such a difference can be clearly resolved. Thus, a final-state resonance is not the source of the strong photoexcitation in the data for $p$-polarized light of energy less than $\hbar\omega = 15$ eV. Similar considerations allow one to exclude band structure effects as the cause of the intense photoionization below $\hbar\omega_p$. Calculations show that the photoemission final states lie in a band gap over the entire range of the data.[34–36]

A difference between "bulk" and "surface" photoexcitation is expected in a single-particle model because of the differences between surface and bulk densities of states.[37] Of particular importance are final-state surface resonances[38,39] which can produce structure in the photoionization cross section[40] similar to that seen in Figs. 3 and 6. We have seen no evidence for such resonances at the photon energies and angles at which our data was taken in either the primary or secondary[40] electrons. This is consistent with single-particle calculations[41,42] which produce partial photoionization cross sections of the surface state and Fermi level of Al(001), which are structureless as a function of photon energy.

Our data differ from the results of other authors in the region of the surface plasmon, $\hbar\omega_{sp} = \hbar\omega_p/\sqrt{2} = 10.5$ eV.[10,14–16,24] A strong enhancement of the photocurrent has been seen near the surface-plasmon energy in other studies of photoemission from aluminum in which the question of intensities has been addressed,[10,14–16,24] while there is at most a shoulder in our data near $\hbar\omega_{sp}$ (Fig. 6). Light can couple to surface plasmons only through surface roughness.[43] A surface may be smooth over distances of a few hundred angstroms yet still have strong optical coupling to surface plasmons.[44] Since typical low-energy electron diffraction (LEED) instruments have inherent coherence lengths of $\sim 100$ Å (Ref. 45) one may have reasonably sharp LEED spots from a sample which is sufficiently rough for appreciable coupling to surface plasmons. While it is well known that the optical excitation of plasmons on a rough surface is different for $s$- and $p$-polarized light,[46,47] the data for $s$-polarization (Fig. 2) should also show some effect due to surface plasmons if the surface is sufficiently rough. Certainly no enhancement was seen, as the signal became very small for $s$-polarized light and $\hbar\omega < 11$ eV. It is clear that the effects we are observing are characteristic of smooth surfaces and are not the result of surface roughness.

Up to this point we have described the data in Fig. 6 below $\hbar\omega = 15$ eV as enhanced relative to the other data. Without further evidence one might well argue that the photoionization cross sections from aluminum are suppressed except for certain photon energies and experimental geometries. In order to remove any remaining uncertainties in our interpretation of the data we have made an absolute calibration of the photoemission cross sections. To our knowledge, this is the first absolute determination of photoionization cross sections from single initial state at a surface.

The absolute measurements were made by mounting a movable Faraday cup into our vacuum chamber which had the same collection geometry as our electron energy analyzer. The current collected in the Faraday cup equalled the total integrated area under an energy distribution curve. This provided an absolute calibration for the photocurrent. At $\hbar\omega = 13$ eV, the measured Fermi-level normal-emission cross section for $p$-polarized incident light was found to be $10 \times 10^{-4}$ electrons/photon eV sr. Because of experimental uncertainties, this result is uncertain to within a factor or 2. A comparison of our measured cross sections with theoretical results will be given in the next section.

The question naturally arises as to whether the effects of a spatially varying photon field in the surface region can influence the photoemission from adsorbates. Since the dominant effect occurs below $\hbar\omega = 15$ eV, only states with low binding energy can be detected at these photon energies. Most adsorbates have relatively large binding energies. It was nevertheless possible to determine if the effect remains by remeasuring the Fermi-level and surface-state cross sections for an Al(001) crystal which has an overlayer of oxygen.

The enhancement of the photo-excitation cross section when $\hbar\omega < \hbar\omega_p$ still occurs for an oxygen-covered Al(001) crystal, as seen in Fig. 7. The aluminum was exposed to 100 L (langmuir) of oxygen, which produces approximately one monolayer of oxygen or oxide.[48,49] The data in Fig. 7 are in the same units as all other figures of Al cross sections in this paper. An overall reduction of photoionization intensity is seen at all photon energies but the spectral profile is approximately the same as for clean aluminum. It appears that the data in the region $\hbar\omega \lesssim 11$ eV is relatively enhanced for the oxygen-covered aluminum as compared to the clean Al data. This suggests that the oxygen is causing some surface inhomogeneities leading to the excitation of surface plasmons. Since the dielectric response is seen to affect the photoemission even with an oxygen overlayer, the intensities of photoexcitation from adsorbed layers could be also affected. The enhancement of the photoionization cross section is a consequence of the abrupt transition between vacuum and solid and is independent of the details of the surface electronic structure, to some extent.

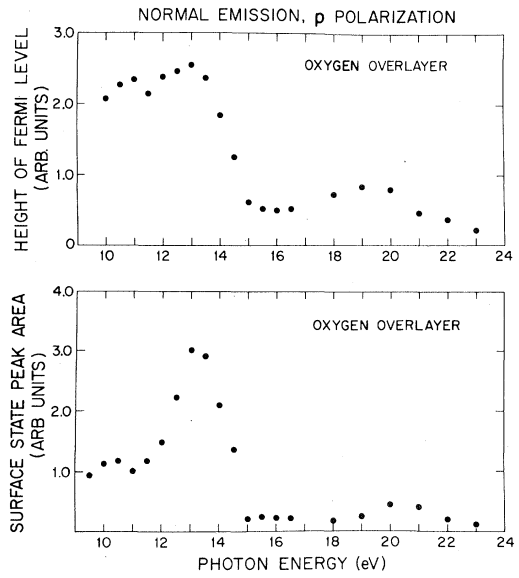


FIG. 7. Normal-emission Fermi-level and surface-state cross sections for aluminum with an oxygen overlayer. The incident light is 45° incident and the $\vec{A}$ vector lies in the (110) plane.

In this section we have presented data which show a strong enhancement of photoionization cross sections from aluminum for $p$-polarized light and excitation energies below the bulk plasmon energy. The energy- and angle-resolved nature of the data enables one to conclude unambiguously the following: (1) The mechanism which results in the enhanced photoexcitation is surface related. (2) It is *not* an immediate consequence of the surface density of state or bulk band structure. (3) The effect is correlated with the excitation frequency but cannot be explained in terms of the bulk dielectric response. A theory which can quantitatively account for the observed enhancement is presented and discussed in the next section.

## III. THEORY

The arguments concerning the nature of the electromagnetic field in the surface region which were presented in the Introduction form a useful guide for determining whether dielectric response will have a strong effect on surface photoemission. However, these arguments ignore nonlocality, which has a significant effect on the fields quantitatively, and are not self-consistent, a more fundamental objection. This latter problem may be seen as follows. A zero in the real part of the local dielectric function will lead to sharp peaks in the electromagnetic fields in the surface region. These rapidly varying fields will, in turn, result in enhanced photoabsorption. This would imply a significant imaginary

component in the dielectric function in the surface region. This interplay between the dielectric functions, the electromagnetic fields determined by the system's dielectric properties, and the resulting photoabsorption requires a self-consistent theory. Formalisms such as the random-phase approximation, in which the dielectric function are directly determined from the excitations of the system, are particularly appropriate. As the results of a proper calculation show (Fig. 8), the surface peak in the self-consistently determined electromagnetic field occurs in the *imaginary* part of the field. A similar effect is known to occur in atomic photoabsorption.[50]

The specification of the electronic states of a system by single-particle orbitals necessitates the use of an effective radiation field to describe photoionization cross sections properly. In order to understand the manner in which many-body effects may be incorporated in an effective perturbing field it is useful to confine the discussion to a specific model. Density-functional formalism in the local density approximation[52] is particularly convenient.

An electromagnetic field incident on a given system will induce an average current density $\delta n(\vec{r},\omega)$.

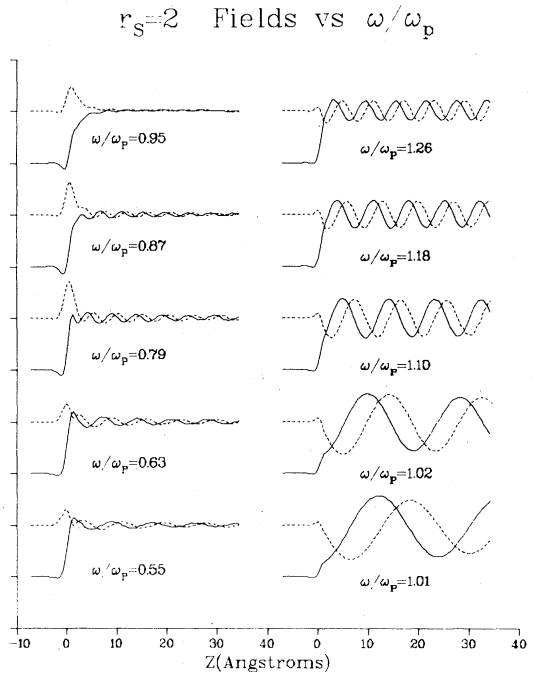


FIG. 8. Calculations by Feibelman (Ref. 51) for the real (solid lines) and imaginary (dashed lines) parts of $[A_z(z)/A_{z,i}-1]/[1-\epsilon(\omega)]$ for a jellium surface ($r_s = 2$), where $A_{z,i}$ is the classical field inside the solid. Note the peak in the imaginary part of the field for $\hbar\omega < \hbar\omega_p$. The vacuum is for $z < 0$, the solid is in the half-space $z > 0$.

An electron in a single-particle orbital will "see" the resulting induced Coulomb interaction and exchange-correlation potential as well as the incident field. It should be noted that this effective field differs slightly from the field that is a solution to Maxwell's equations. The Maxwell field is the one seen by a test charge which is distinguishable from the electrons in the system and therefore does not include the exchange-correlations terms. The effects of the induced exchange and correlation have been found to be small,[50] and the neglect of this term is justified in our discussion.

Various theoretical models have been used to investigate the nature of the microscopic Maxwell fields at the surface of a metal.[51,53–55] The calculations of Feibelman,[51] in which the surface potential barrier is treated realistically, are in particularly good agreement with our data. The equation which Feibelman solves in order to obtain the Maxwell fields in the surface region may be found as follows. The continuity equation for current $\vec{j}$ and charge density $\rho$,

$$\vec{\nabla}\cdot\vec{j} + \frac{\partial\rho}{\partial t} = 0 \ , \tag{5}$$

Gauss's law,

$$\vec{\nabla}\cdot\vec{E} = \vec{\nabla}\cdot\left[\frac{1}{c}\frac{\partial\vec{A}}{\partial t}\right] = 4\pi\rho \ , \tag{6}$$

and Ohm's law,

$$\vec{j}(\vec{x}) = \int \vec{\sigma}(\vec{x},\vec{x}')\cdot\vec{E}(\vec{x}')dx' \ , \tag{7}$$

where $\sigma(\vec{x},\vec{x}')$ is the nonlocal conductivity tensor, lead to

$$\vec{\nabla}\cdot\left[\int\vec{\sigma}(\vec{x},\vec{x}')\cdot\vec{A}(\vec{x}')dx' - \frac{i\omega}{4\pi}\vec{A}(\vec{x})\right] = 0 \ . \tag{8}$$

This equation is exact. Assuming all spatial variations parallel to the surface are negligible compared to those perpendicular to the surface, Eq. (8) reduces to a one-dimensional integral equation

$$A_z = A_0 - \frac{4\pi i}{\omega}\int\sigma_{zz}(z,z')A_z(z)dz' \tag{9a}$$

$$= A_0 - \frac{4\pi i}{\omega}\int\sigma_{zz}(z,-q)A_z(q)dq \ , \tag{9b}$$

where $A_0$ is a constant of integration and where $\sigma_{zz}(z,q)$ and $A_z(q)$ are the Fourier transforms of $\sigma_{zz}(z,z')$ and $A_z(z')$, respectively. In the limit $z \to -\infty$ (into the vacuum), $\sigma \to 0$ so that $A_0$ is the (classical) field outside the solid. Equation (9b) ex-

plicitly shows how the field acquires additional Fourier components because of dielectric response. Evaluating $\sigma$ within the random phase approximation, Feibelman has solved Eq. (9a) for light in the ultraviolet. Examples of the computed fields are shown in Fig. 8. The results of the $r_s = 2$ jellium calculations as a function of $\hbar\omega/\hbar\omega_p$ may be compared to the data by renormalizing $\hbar\omega_p$ to the measured value for aluminum of 15 eV.

Using these spatially varying photon fields and the jellium single-particle wave functions, the Fermi-level normal-emission cross section has been calculated and is shown as the solid line in Fig. 6. There is excellent agreement between the theory and experiment. When the photoemission element is evaluated using the applied field, the dashed line in Fig. 6 results. This cross section is much smaller in magnitude than the result obtained using a spatially varying field and must be multiplied by a factor of 10 to be on the same scale as the other results. The two different calculations also yield dissimilar spectral profiles. The single-particle cross section is structureless. This is consistent with the data for *s*-polarized incident light (Fig. 2) in which the general shape of the spectral profile was given by the classical dielectric response, indicating the lack of sturcture in the matrix element. Using the spatially varying photon field the calculated photoionization cross-section at $\hbar\omega = 13$ eV is $7 \times 10^{-4}$ electrons/photon eV sr, compared to the measured value of $10 \times 10^{-4}$ electrons/photon eV sr. We have quantitative agreement with the calculations of Feibelman.

The calculated fields exhibit precisely the features discussed in the begining of this section. A peak in the imaginary part of electromagnetic fields occurs in the surface region when $\hbar\omega < \hbar\omega_p$. Below the plasma frequency (Fig. 8) there are short-wavelength fields extending into the solid. In this spectral range, the condition for a longitudinal field

$$\epsilon_L(q,\omega) = 0 \ ,$$

where $\epsilon_L$ is the longitudinal dielectric constant, is satisfied by a complex value of $q$. Thus, longitudinal fields are confined to the surface region, falling off as $1/z^2$, where $z$ is the distance into the bulk.[52,54] Above the plasmon energy (Fig. 9) one finds optically excited propagating longitudinal fields, i.e., bulk plasmons.

The way in which the microscopic photon field will affect the photoionization cross section can be seen by looking at the integrand of the photoionization matrix element. In the range of photon energies covered by Feibelman's calculations the induced longitudinal fields are not found to contribute appreciably to the cross section. In contrast, the nature of the photon field near $z = 0$ (Fig. 8) significantly affects the photoionization cross section when $\hbar\omega < \hbar\omega_p$.

In addition to the calculations of Feibelman, the surface fields have been studied extensively within the semiclassical infinite-barrier model of the electron gas.[53,55] In these calculations the surface is taken to be an abrupt discontinuity between the vacuum and the electron gas. Accordingly, the structure in $A_z(z)$ found in Feibelman's calculation near $z = 0$ that results from a varying ground-state charge density is not reproduced in the semiclassical infinite-barrier model. Since the photoionization cross section is largely determined by the values of the field near $z = 0$, particularly for $\hbar\omega < \hbar\omega_p$, this latter model is not expected to yield quantitative agreement with experiment. The semiclassical infinite-barrier model does produce the Friedel oscillations that extend several tens of angstroms into the solid, but these appear to have a small effect on photoemission cross section.

For sufficiently large excitation energies ($\hbar\omega \gtrsim 20$ eV for aluminum) the optically excited plasmons can decay into particle-hole pairs. The fields in the surface region have been calculated in this photon energy range in the semiclassical infinite-barrier model and an enhancement of the total photoyield has been predicted. We have seen no enhancement of the photoionization cross section of either the Fermi level of surface state above 20 eV, showing that *surface* photoexcitation is not strongly effected by optically excited *bulk* plasmons. Optically excited bulk plasmons which have wavelengths much shorter than transverse electromagnetic waves could result in nonvertical transitions, smearing out bulk transitions. They may be the reason that direct transitions are seldom seen in Al for *p*-polarized light with $\hbar\omega < 30$ eV.[56] At sufficiently high photon energies the plasmons are damped and peaks due to direct transitions excited by perpendicular field components can again be clearly seen in the spectra.[56] The theory and our data are by no means inconsistent.

## V. CONCLUSION

The results presented and discussed in this paper have shown unambiguously that a single-particle picture is inadequate to describe surface photoemission. The electronic levels may still be taken as

TABLE I. The plasmon energies are defined as the peak positions of Im $(-1/\epsilon)$. There is additional structure in the loss function in Cu and Ni due to interband transition, and this could have an effect on the dielectric response in the surfaces of these metals.

| Material | Plasmon energy (eV) | References |
|---|---|---|
| Mo | 24.4 | 57 |
| W | 25.3 | 58 |
| Cu | 19.3 (27.2) | 59 |
| Ni | 21.0 (26.9) | 59 |
| Si | 16.5 | 60 |
| GaAs | 15.8 | 61 |

single-particle states but the effective photon field must include dielectric response, and this may be appreciable. Below $\hbar\omega_p$ the photoexcitation process is dominated by many-body effects, while at higher photon energies photoionization is well described by single-particle models. In particular, no contribution to surface photoexcitation by induced longtiudinal fields has been observed. The effect remains when there is an adsorbed overlayer. Since spatial variations in the photon field are significant only for components of the vector normal to the surface, the dielectric response will have a significant effect on angular distributions at appropriate photon energies.

Aluminum was chosen as the metal with which to establish the existence of the many-body effects and elucidate some of its basic properties because it is a simple metal, leading to a reasonably straightforward interpretation of the data. Effects similar to those presented here for aluminum might occur for other materials whenever the excitation light is in the region of the bulk plasmon. Typical plasmon energies are given in Table I. The manner in which these effects might appear in more complex solids, such as transition metals and semiconductors, is not obvious. Special profiles of photoemision cross-sections from surface state on Mo(001) and W(001) (Ref. 40) are similar to those reported in this paper for aluminum. The data in Ref. 40 are complicated by the existence of final state resonances which contribute, at least in part, to the enhancement of the surface-state cross sections below $\hbar\omega_p$.[40] Different experimental geometries may lead to more conclusive results for the refractory metals.

Damping due to interband transitions, while playing a negligible role in aluminum, would be expected to be of some importance in $d$-band metals. The peak in the photon field near $z = 0$ will be significantly diminished in intensity when the bulk dielectric constant acquires a substantial imaginary part. The longitudinal fields will also be damped. Neverthless, simple classical considerations indicate that surface dielectric response will be important in non-nearly-free-electron metals.[62] Determination of the effect of spatially varying photon fields on photoemision form transition metals and semiconductors is therefore necessary in order to unambiguously interpret intensity profiles from these materials.

## ACKNOWLEDGMENTS

We would like to thank Dr. Peter J. Feibelman and Dr. J. B. Pendry for providing us with the results of their calculations. The work was supported by the National Science Foundation—Materials Research Laboratory Grant No. DMR-79-23647. The Synchrotron Radiation Center of the University of Wisconsin was supported by National Science Foundation Grant No. 74-15098.

*Present address: Dept. of Physics, University of California, Berkeley, CA 94720.

[1]Preliminary accounts of our results have been published in Harry J. Levinson, E. W. Plummer, and Peter J. Feibelman, Phys. Rev. Lett. 43, 952 (1979); J. Vac. Sci. Technol. 17, 216 (1980).

[2]See H. A. Bethe and E. E. Salpeter, *Quantum Mechanics of One and Two Electron Atoms,* (Springer, Berlin, 1957). Throughout this paper the radiation field will be given in the temporal gauge (scalar potential is identically zero). Since our results will be discussed in terms of exact many-body wave functions of the eigenstates of a single-particle Hamiltonian the conclusions are gauge independent.

[3]H. Ehrenrich and M. H. Cohen, Phys. Rev. 115, 786 (1959).

[4]R. E. B. Mackinson, Proc. R. Soc. London Ser. A 162, 367 (1937).

[5]L. D. Laudau and E. M. Lifshitz , *Electrodynamics of Continuous Media,* (Pergamon, New York, 1960), Sec. 68.

[6]K.L. Kliewer and Ronald Fuchs, Phys. Rev. 172, 607 (1968).

[7]These induced fields in the surface region are not, strictly speaking, surface plasmons. A plasmon is a collective mode which may exist independently of the perturbation responsible for its excitation, while the longitudinal field discussed here would vanish if the incident field were removed. Optical coupling to surface plasmons may occur only through surface roughness.

[8]A. G. Hill, Phys. Rev. 53, 184 (1938).

[9]H. Mayer and H. Thomas, Z. Phys. 147, 419 (1957).

[10]J. G. Endriz and W. E. Spicer, Phys. Rev. Lett. 27, 570 (1971).
[11]S. A. Flodström and J. G. Endriz, Phys. Rev. Lett. 31, 893 (1973).
[12]J. Monin and G. A. Boutry, Phys. Rev. B 9, 1309 (1974).
[13]S. A. Flodström and J. G. Endriz, Phys. Rev. B 12, 1252 (1975).
[14]S. A. Flodström, G. V. Hansson, S. B. M. Hagström, and J. G. Endriz, Surf. Sci. 53, 156 (1975).
[15]Helmuth Petersen and S. B. M. Hagström, Phys. Rev. Lett. 41, 1314 (1978).
[16]Helmuth Petersen, Z. Phys. B 31, 171 (1978).
[17]G. Jezequel, in Conference Proceedings of the 6th International Conference on VUV Physics, 1980 (unpublished), pp.1 – 58; Phys. Rev. Lett. 45, 1963 (1980)
[18]G. N. Berglund and W. E. Spicer, Phys. Rev. 136, A1030 (1964).
[19]G. D. Mahan, Phys. Rev. B 2, 4334 (1970).
[20]C. L. Allyn, T. Gustafsson, and E. W. Plummer, Rev. Sci. Instrum. 49, 1197 (1978).
[21]Brian P. Tonner, Nucl. Instrum. Methods 172, 133 (1980).
[22]L. R. Canfield, R. G. Johnston, and R. P. Madden, Appl. Opt. 12, 1611 (1973).
[23]Syton is a registered trade name of Monsanto.
[24]G. V. Hansson and S. A. Flodström, Phys. Rev. B 18, 1562 (1978).
[25]P. O. Gartland and B. J. Slagsvold, Solid State Commun. 25, 489 (1978).
[26]M. P. Seah and W. A. Dench, Surf. Interface Analysis 1, 2 (1979).
[27]R. W. Ditchburn and G. H. C. Freeman, Proc. R. Soc. London A294, 20 (1966).
[28]H. J. Hagemann, W. Gudat, and C. Kunz, J. Opt. Soc. Am. 65, 742 (1978).
[29]For polarized light, molecular photoionization cross sections are of the form $\frac{d\sigma}{d\Omega} = (\sigma_0/4\pi)[1 + \beta P_2(\cos\theta)]$, where $\theta$ is the angle between the light vector and the momentum of the photoelectron and $-1 \leq \beta \leq 2$. Only for $\beta = 0$ will the emission be isotropic, while maximal anisotropy ($\beta = 2$) will occur for a plane wave final state. See, for example, J. Cooper and R. Zare, J. Chem. Phys. 48, 943 (1968).
[30]H. Puff, Phys. Status Solidi 1, 636 (1961).
[31]J. K. Sass, Surf. Sci. 51, 199 (1975).
[32]P. Oelhafen, U. Gubler, and F. Greuter, in *Electrons in Disordered Metals and at Metallic Surfaces.* edited by P. Phariseau, B. L. Gyorffy, and L. Scheive (Plenum New York 1979).
[33]W. L. Schaich and N. W. Aschroft, Solid State Commun. 8, 1959 (1970).
[34]S. P. Singhal and J. Callaway, Phys. Rev. B 16, 1744 (1973).
[35]V. Hoffstein and D. S. Boudreaux, Phys. Rev. B 2, 3013 (1970).
[36]V. Moruzzi, J. F. Janak, and A. Williams, *Calculated Electronic Properties of Metals* (Pergamon, New York, (1980).
[37]David Kalkstein and Paul Soven, Surf. Sci. 26, 85 (1971).
[38]E. G. McRae, Rev. Mod. Phys. 51, 541 (1979).
[39]R. Z. Bachrach, D. J. Chadi, and A. Bianconi, Solid State Commun. 32, 249 (1977).
[40]Shang-Li Weng, E. W. Plummer, and T. Gustafsson, Phys. Rev. B 18, 1718 (1978).
[41]J. B. Pendry and J. F. L. Hopkinson, J. Phys. (Paris) Colloq. 7, C4-142 (1978).
[42]J. B. Pendry (private communication).
[43]H. Raether, in *Physical of Thin Films*, edited by George Hass, Maurice H. Francombe, and Richard W. Hoffman (Academic, New York, 1977), Vol. 9.
[44]J. Crowell and R. H. Ritchie, J. Opt. Soc. Am. 60, 794 (1970).
[45]Robert L. Park, J. E. Houston, and D. G. Achreiner, Rev. Sci. Instrum. 42, 60 (1971).
[46]Dwight W. Berreman, Phys. Rev. 163, 855 (1967).
[47]D. Beaglehole and O. Hunderi, Phys. Rev. B 2, 309 (1970).
[48]R. Michel, C. Hourdan, J. Castaldi, and J. Derrien, Surf. Sci. 84, L509 (1979).
[49]C. W. B. Martinson, S. S. Flodstrom, J. Rundgren, and P. Westrin, Surf. Sci. 89, 102 (1979).
[50]A. Zangwill and Paul Soven, Phys. Rev. A 21, 1561 (1980).
[51]Peter J. Feibelman, Phys. Rev. Lett. 34, 1092 (1975); Phys. Rev. B 12, 1319 (1975).
[52]W. Kohn and L. J. Sham, Phys. Rev. 140, A1133 (1965).
[53]K. L. Kliewer, Phys. Rev. B 14, 1412 (1976); 15, 3759 (1977).
[54]G. Mukhopadhyay and S. Lundqvist, Solid State Commun. 21, 629 (1977); Phys. Scr. 17, 69 (1978).
[55]P. Apell, Phys. Scr. 17, 535 (1978).
[56]Harry J. Levinson, F. Greuter, and E. W. Plumer, unpublished.
[57]J. H. Weaver, D. W. Lynch, and C. G. Olsen, Phys. Rev. B 10, 501 (1974).
[58]J. H. Weaver, D. W. Lynch, and C. G. Olsen, Phys. Rev. B 12, 1293 (1975).
[59]D. L. Misell and A. J. Atkins, Philos. Mag. 27, 95 (1973).
[60]T. Aiyama and K. Yada, J. Phys. Soc. Jpn. 36, 1554 (1974).
[61]R. Manzke, J. Phys. C 13, 911 (1980).
[62]Amitabha Bagchi and Nikhiles Kar, Phys. Rev. B 18, 5240 (1978).